One-dimensionality of phonon transport in cup-stacked carbon nanofibers

2010 J. Phys.: Condens. Matter 22 065403

(http://iopscience.iop.org/0953-8984/22/6/065403)

J. Phys.: Condens. Matter **22** (2010) 065403 (6pp) doi:10.1088/0953-8984/22/6/065403

One-dimensionality of phonon transport in cup-stacked carbon nanofibers

Y Ito, M Inoue and K Takahashi

Department of Aeronautics and Astronautics, Kyushu University, 744 Motooka, Nishi-ku, Fukuoka 819-0395, Japan

E-mail: takahashi@aero.kyushu-u.ac.jp

Received 23 October 2009, in final form 5 January 2010
Published 22 January 2010
Online at stacks.iop.org/JPhysCM/22/065403

Abstract

We treat the ballistic heat conduction of cup-stacked carbon nanofibers (CSCNF) by a nonequilibrium molecular dynamics simulation. The CSCNF consist of numerous tiny graphene cups linked in line by weak intermolecular forces. The simulation results show that the thermal conductivity varies with the fiber length in a power law fashion with an exponent as large as 0.7. The calculated phonon density of states revealed that a low frequency oscillation in the radial and axial directions dominates the heat conduction in CSCNF. The atomic motions indicate that these low frequency oscillations are quasi-one-dimensional (1D) where each cup moves axially like a rigid body and radially with a breathing motion. This quasi-1D oscillation occurs due to the unique structure of a CSCNF that resembles a 1D harmonic chain. Our investigations show that treating a CSCNF as a 1D chain with three-dimensional oscillations explains why this material has the highest ballistic phonon transport ever observed.

1. Introduction

In the past three decades, many superior properties of the carbon nanotube (CNT) have been extensively studied. Its extremely high thermal conductivity has been revealed both experimentally [1–5] and theoretically [6–8] to be as high as 4000 W m^{-1} K^{-1} for a single-walled nanotube (SWNT) at room temperature [8]. This excellent heat transport ability is attributed not only to the stiff sp^2 bond but also to the long mean free path (MFP) of a phonon. In pristine SWNTs, boundary scattering of phonons does not occur and only the phonon–phonon scattering limits the phonon mean free path (MFP). This type of scattering can be expected to be less in SWNTs than any other material due to their quasi-one-dimensionality, resulting in a long MFP of the order of micrometers even at room temperature. When the MFP is longer than the material's length, the phonon is scattered at the ends and the material's thermal conductivity is changed. Maruyama [9] discovered that, for a short SWNT, the long MFP of a pristine SWNT yields a unique thermal conductivity λ that depends on the tube length L as $\lambda \propto L^{\alpha}$. Here, the phonon is scattered by the tube ends. This is in contrast to the usual Fourier law situation, where the thermal conductivity of materials is constant. The power law variation of thermal conductivity is known as ballistic phonon transport.

On the other hand, it has been disclosed that unusual thermal conduction appears in 1D systems [10]. Rieder *et al* reported that the 1D harmonic chain shows a flat temperature distribution even though a temperature difference is applied to its ends [11]. This is because the phonon in this system is transported without scattering, which results in the exponent $\alpha = 1.0$. As computational power is improved, numerical studies are being widely conducted on the heat conduction in 1D chains. Lepri *et al* [12] reported that the thermal conductivity of the anharmonic Felmi–Pasta–Ulam (FPU) β lattice varies with length as $\lambda \propto L^{0.37}$. The FPU α lattice [13] and the Toda lattice [14] have also been investigated and similar power laws were obtained with α values of about 0.4. The 1D harmonic chain with a three-dimensional (3D) oscillation was also treated [15] and its thermal conductivity was found to depend again on a power law with an exponent α within the range 0.55–1.0, corresponding to the degree to which the 3D oscillation is not considered to be not local ($\alpha = 0.55$) or strictly local ($\alpha = 1.0$).

The SWNT is the lowest-dimensional material ever discovered and the length dependence of its thermal conductivity is one of the hottest topics in the heat-related sciences. There are several reports [9, 16, 17] on the value of the exponent α, for example, $\alpha = 0.40$ at 300 K and $\alpha = 0.26$ at 800 K for a (5, 5) SWNT [16]. Recently, a couple

of experimental attempts [18, 19] were conducted to explore the length dependence of a CNT's thermal conductivity, and it was confirmed to increase with its length. However, at variance with the theoretical 1D predictions, it was found that this length dependence holds only for short tubes, and a transition from ballistic to diffusive transport appears as the tube length increases [8, 20]. For an infinitely long SWNT, the thermal conductivity becomes constant because the MFP is shorter than the tube length and the phonon is scattered by the phonon–phonon scattering, not by tube ends. However, if we could discover another truly 1D material, or a more strictly one-dimensional material than a SWNT, then ballistic heat conduction might be realized over a longer distance than so far achieved.

In recent experiments by the authors, an unexpectedly high thermal conductivity of an individual CSCNF was measured [21]. The CSCNF are constructed by stacking truncated cone cups [22]. Only weak intermolecular forces provide the connection between cups. Therefore, the in-axis thermal conduction in a CSCNF had been predicted to be very low based on the usual assumption that the thermal conductivity is independent of the length. However, a value of about 40 W m^{-1} K^{-1} at 300 K was obtained in experiment, even though the reported graphite c-axis thermal conductivity is only 2 W m^{-1} K^{-1} [23]. A theoretical study suggests an even lower thermal conductivity [24]. We have to conclude that the measured thermal conductivity of CSCNF cannot be explained by diffusive heat transfer. The most likely explanation is that unsuspected 1D phonon transport appears in the CSCNF. In this study, in order to make clear the origin of heat conduction of CSCNF, we have conducted nonequilibrium molecular dynamics simulations.

2. Numerical modeling

The calculation model is illustrated in figure 1, together with a high resolution transmission electron micrograph (HRTEM) image of a CSCNF. Although samples we have prepared and measured in the past [21] had outer and inner diameters of approx. 180 nm and 140 nm and lengths of approx. 5 μm, much thinner CSCNFs can be synthesized [22]. Due to the limitations of computational power, we here treat very thin and short samples to understand the fundamental mechanism of phonon transport. Each cup in figure 1 consists of 470 carbon atoms; only carbon hexagons exist in this structure. The cup is part of a graphene cone made up of a circular sector with a central angle of 120° with a radius of 3.49 nm. The outer diameter of a cup is 2.33 nm and the inner is 0.73 nm. The angle between the cup surface and the fiber axis is 19.5° and the axial cup–cup distance is 1.01 nm, as the initial interlayer cup–cup distance is set to 0.337 nm. The Brenner potential [25] is used for the carbon–carbon bond in each cup and the Lennard-Jones potential:

$$\phi(r) = 4\varepsilon\left[\left(\frac{\sigma}{r}\right)^{12} - \left(\frac{\sigma}{r}\right)^{6}\right] \tag{1}$$

for carbon–carbon nonbonded interactions. The parameterization employed for the Lennard-Jones potential in this study is

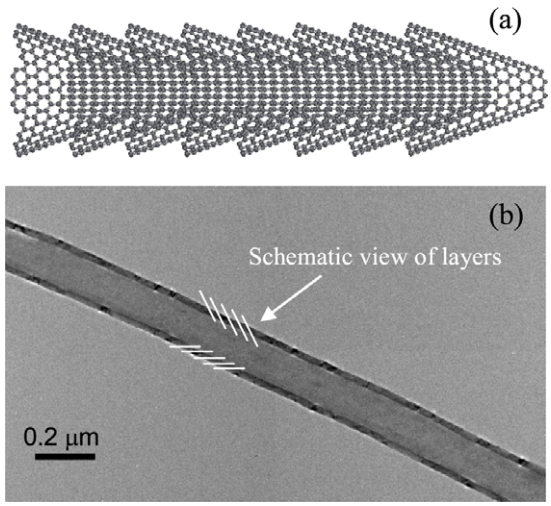

Figure 1. The calculation model (a) and an HRTEM image (b) of a CSCNF. In the calculation model, the outermost regions have imposed on them a fixed boundary condition. Their neighboring small regions are set to be a heat bath. The temperature of the left heat bath is set to 320 K and that of the right is 280 K. Panel (b) shows the hollow configuration of an actual CSCNF. A schematic view of the layers in a CSCNF is also shown in (b).

$\varepsilon = 2.40$ meV and $\sigma = 0.337$ nm. A fixed boundary condition is imposed on the end regions. Their neighbor regions comprise a heat bath, whose temperature is controlled by a Nose–Hoover thermostat [26]. In this simulation, the velocity Verlet method is adopted to integrate the equation of motion with a step time of 0.5 fs. For the first 500 ps, the simulations begin by equilibrating the system at 300 K. The temperature is calculated using the kinetic theorem as follows:

$$T = \frac{1}{3nk_{\mathrm{B}}}\sum_{i=1}^{n} m_i v_i^2, \tag{2}$$

where n is the number of molecules which belong to a small region, k_{B} is the Boltzmann constant, m_i is the mass and v_i is the velocity of the ith molecule. In the current study, the left heat bath is raised to 320 K and the right heat bath is lowered to 280 K. We treated CSCNFs made up from three, five and eight cups.

3. Thermal resistance

For this kind of 1D material, the cross-sectional area needed to obtain the thermal conductivity is sometimes difficult to define, but the thermal resistance R is straightforwardly calculated from $R = \Delta T/Q$, where ΔT is the temperature difference between both heat baths and Q is the heat flow calculated from the average of the additional kinetic energy between the left and right heat baths. The thermal resistance in this way is 1.04×10^{10} K W^{-1} for a three-cup CSCNF and 1.29×10^{10} K W^{-1} for one of five cups; the thermal resistance does not increase in proportion to the number of interlayers, in disagreement with the prediction that the total resistance should be the summation of interlayer resistances. For eight cups, the thermal resistance is 1.64×10^{10} K W^{-1}. Here, the

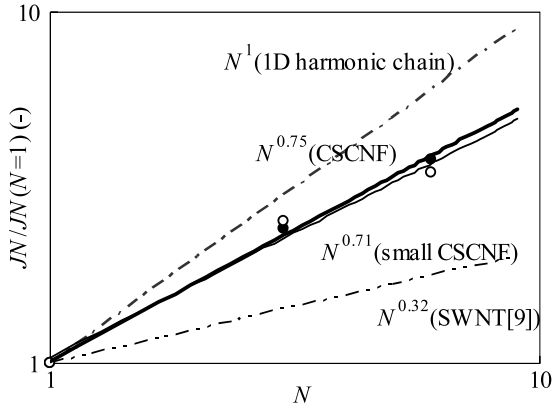

Figure 2. The N dependence of JN (made dimensionless by dividing by JN ($N = 1$)) of a CSCNF, where N is the number of free cups and J is the heat flux. The thick line represents a $N^{0.75}$ variation and the thin line, one of $N^{0.71}$. The slope corresponding to a one-dimensional harmonic chain (dotted–dashed line) and an SWNT [9] (double-dotted–dashed line) are also plotted. The product JN is proportional to the thermal conductivity λ and N is proportional to the length L. Circles represent calculated data for three, five and eight cups CSCNFs.

N dependence of JN of the CSCNF is plotted in figure 2, where N is the number of free cups and J is the heat flux. The product JN is made dimensionless by dividing by JN ($N = 1$). The circle points are the calculated values for the CSCNF in this study. The solid circle is for a 470-atom cup and the open circle is for a 282-atom cup. The lines for a one-dimensional harmonic chain and an SWNT [9] are also plotted for reference. Because JN is proportional to the thermal conductivity λ and N is proportional to the fiber length L [15], the calculated relationship of $\lambda \propto L^{0.32}$ of an SWNT is presented in this plot as the line $JN \propto N^{0.32}$. The relationship between λ and L for a 1D harmonic chain is presented in this plot as $JN \propto N^1$.

The power law exponent α, equal to the slope of a line in figure 2 obtained from the calculated data (circles), for a CSCNF of up to eight cups is 0.75, which means that the phonon transport in a CSCNF has the potential to be more ballistic than in an SWNT. Another CSCNF made from smaller cups, each with the same inner diameter but consisting of 282 atoms, was also investigated. We obtained $\alpha = 0.71$ for this smaller cup. Considering the calculation uncertainty, we consider that the length dependence of thermal conductivity of a CSCNF is essentially independent of cup size.

Concerning the thermal conductivity, our calculations give an extremely low value of 0.112 W m^{-1} K^{-1} for the five-cup system of 5.55 nm length, due to the weak cup–cup interaction. However, the power law ($\lambda \propto L^{0.75}$) found for this CSCNF predicts that it will overtake the SWNT [8] in terms of heat transport ability if the CSCNF is longer than 6.6 mm at room temperature. Thus, the exponent α, or the one-dimensionality of heat conduction, is critical for long-distance heat transport.

4. Modal analysis

The phonon density of state (DOS) is calculated for a five-cup CSCNF using all the atoms in a cup, except for the fixed and heat-bath atoms by the following equation:

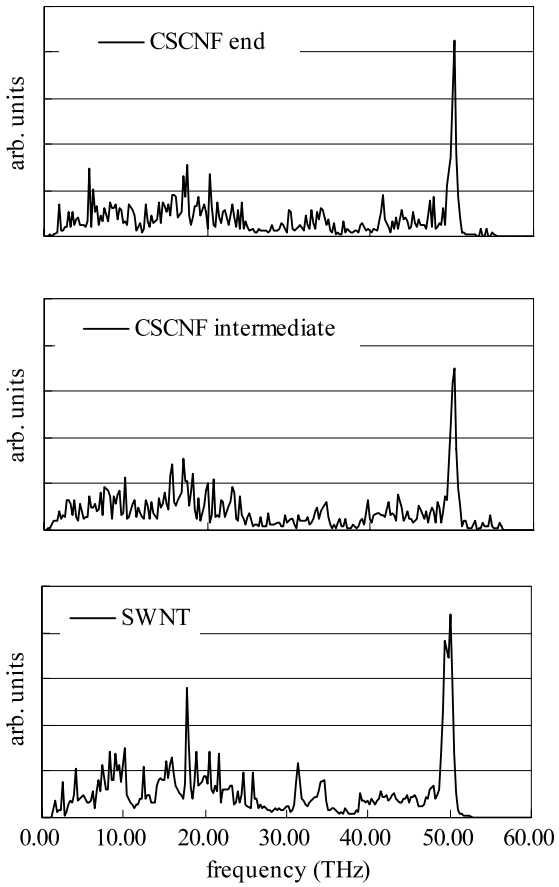

Figure 3. DOS of the left end fixed cup, intermediate cup and a (5, 5) SWNT from 0 to 60 THz. The resolution is 0.25 THz. An oscillation attributed to the presence of carbon hexagons appears in all graphs.

$$D(\omega) = \int e^{iwt} \langle v(t) \cdot v(0) \rangle \, dt, \tag{3}$$

where ω is frequency. The DOSs of the end cup, an intermediate cup and an SWNT are displayed in figure 3, covering a range from 0 to 60 THz with a resolution of 0.25 THz. All the DOSs are similar because both a CSCNF and an SWNT are graphene-based tubular materials and the oscillations attributed to the carbon hexagons always appear. The stiff bonding force in graphene produces high frequency phonons [27], but such phonons are not propagated through the cup interlayers because the cup–cup connection is only made by very weak van der Waals' forces. Extremely low frequency oscillations exist only in the intermediate cup. The heat conduction of the CSCNF along with the fiber axis is considered to be carried by lower frequency phonons.

In order to discuss the low frequency oscillation, the DOSs are recalculated from 0 to 2 THz with a resolution of 0.01 THz in the axial, circumferential and radial directions. Figure 4(a) shows DOS of the left end cup and (b) is that of its neighbor on the right. Figure 4(c) is for the center one of a five-cup CSCNF. While low frequency peaks around 1 THz are not apparent in the end cup, the intermediate cups have several peaks in the

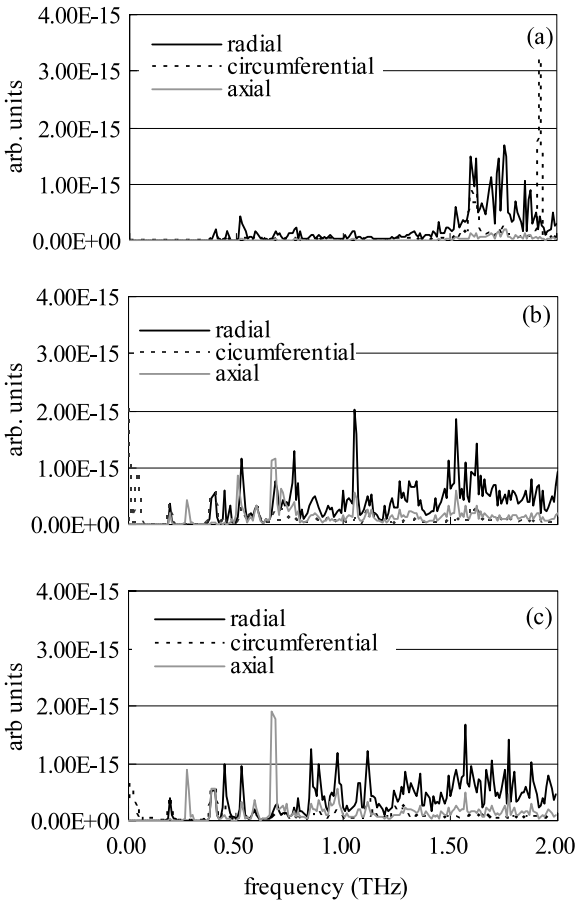

Figure 4. DOS from 0 to 2 THz in the axial (solid gray), circumferential (broken black) and radial (solid black) directions for the first (a), the second (b) and the third (c) cup. The resolution is 0.01 THz. The first cup, upon which a fixed condition is imposed, has a different distribution from the others, which are similar. For all cups, the circumferential component is weak. The axial and radial components are dominant below 1.00 THz, while the axial is dominant at frequencies higher than 1.00 THz.

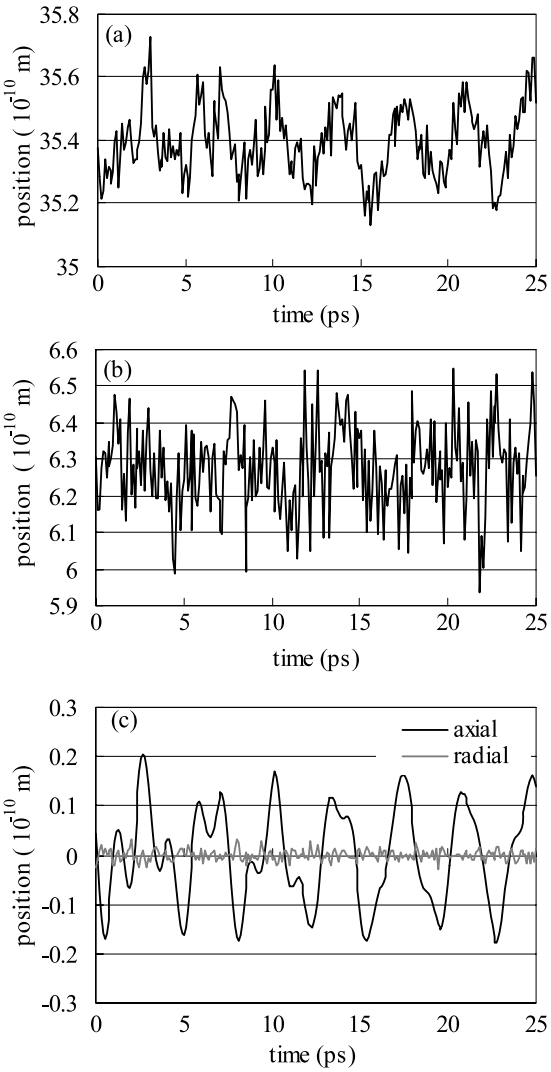

Figure 5. The displacement in time of a carbon atom and the center of inertia of the third cup in axial and radial directions. The vertical axis indicates the displacement from the time-averaged position of the center of inertia. The horizontal axis is time with a resolution of 0.1 ps. (a) The axial displacement of a carbon atom. (b) The radial displacement of a carbon atom. (c) The axial and radial displacement of the center of inertia of the cup. Panels (a) and (b) show the real position of a carbon atom in the third cup. In (c), the black line shows the axial displacement, and the gray line shows the radial. The resolution is 0.1 ps. Both phase and amplitude are almost the same for the center of inertia of the cup and an atom in the cup. The radial displacement of (b) is considered to be due to a breathing-like mode.

range of 0.2–1.5 THz; these are expected to be the major heat carrier of a CSCNF.

Compared with the other directions, the circumferential oscillation is largely absent except for a peak at 2 THz for the end cup. This peak is due to a twist mode. Because the intermediate cups are connected by nonbonding forces and can freely rotate, this twist mode does not propagate and only a very slow rotation of intermediate cups occurs. As a result, the contribution of the circumferential mode to the heat conduction is negligible. For axial and radial modes, the DOSs of intermediate cups in figures 4(b) and (c) are similar. The low frequency oscillations in these directions are thought to dominate heat conduction in CSCNF.

5. One-dimensionality of CSCNF

A CSCNF is made up from nonbonded cups that are stiff structures of covalently bonded carbon atoms. Thus, it is meaningful to investigate our MD results by assuming each cup to be a rigid body. Figure 5 shows the axial (a) and radial (b) motions of an atom and those of the center of inertia (c) of the third cup. The oscillation with a frequency up to 10 THz can be observed in figure 5. This figure allows us to discuss the motions which are important contributors to heat conduction in the CSCNF. For the oscillation in the axial direction, the cup motion in figure 5(c) shows good agreement with the motion of a carbon atom in figure 5(a). This means that both phase and amplitude are almost the same for all atoms in a cup, resulting in a rigid-body-like motion of cups in the axial direction. On the other hand, the radial displacement of the center of inertia is smaller than 0.03×10^{-10} m, though that of an atom in figure 5(b) is

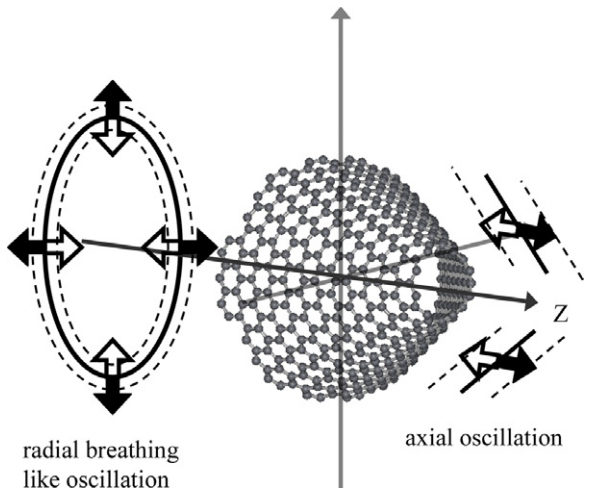

Figure 6. A schematic view of the radial breathing-like mode and the axial mode. The solid line shows the equilibrium position and the distance between broken lines shows the amplitude. The cup oscillates backwards and forwards in the axial direction or deforms radially between the solid and broken lines. The off-axis motion rarely appears in a CSCNF.

about 0.5×10^{-10} m. This suggests that each cup moves in a breathing-like way in the radial direction. In other words, as figure 6 illustrates, the cup diameter repeatedly expands and contracts, and an off-axis motion rarely appears. Because this coherent breathing [28] coupled with axial and radial motions is expected to be responsible for the one-dimensionality of CSCNF, we discuss it further in the following sections.

Considering that the cup surface is at an angle of about 9.59° with the fiber axis, this breathing-like radial mode can be divided into interlayer and in-layer modes as well as the axial oscillation. Roughly speaking, the interlayer mode coincides with the longitudinal mode of a 1D chain and the in-layer mode with the transverse mode. Consequently, the motion of a CSCNF can be regarded as that of a 1D harmonic chain with 3D oscillations. The presence of 3D oscillations is one of the major reasons why α obtained in our simulations is less than 1.0, even though the CSCNF is a very similar system to a 1D harmonic chain.

Liu *et al* [15] treated the 1D harmonic chain with a 3D oscillation and found that α is dependent on the non-dimensional quality $a^*/T^{*0.5}$, where a^* is the dimensionless lattice constant and T^* is the dimensionless temperature. This quantity indicates the relative scale of the lattice oscillation to the lattice constant. A large $a^*/T^{*0.5}$, where the atomic oscillation can be considered as local, induces a large α. When $a^*/T^{*0.5}$ is over 500, α reaches 1.0 and the oscillation is considered as strictly local. When the oscillation cannot be considered as local, that is for $a^*/T^{*0.5} < 10$, α converges to 0.55. By using this quantity, we can evaluate the one-dimensionality of the phonon transport in the present CSCNF. The non-dimensional temperature T^* is expressed as

$$T^* = \frac{k_B}{m\omega_0^2 b^2} \times T, \tag{4}$$

where k_B is the Boltzmann constant, m is the mass of the particle, ω_0 is the oscillation frequency and b is the equilibrium distance [29, 30]. In the current study, b is identical to the lattice constant a, which is also equal to the interlayer distance of cups. Thus, because a^* is expressed as $a^* = a/b$, then a^* becomes 1.0. The dominant frequency of a CSCNF here is the order of 1 THz as discussed earlier. Other parameters are as follows; $m \sim 10^{-23}$ kg for 470 carbon atoms, $\omega_0 \sim 10^{12}$ Hz, $b \sim 10^{-9}$ m, $k_B = 1.38 \times 10^{-23}$ J K^{-1}, $T = 300$ K. Using these value, the value of the quantity $a^*/T^{*0.5}$ obtained for a CSCNF is about 50, thus the oscillation of the CSCNF can be regarded as quasi-local. Further, the value of $\alpha = 0.75$ obtained for a CSCNF matches the α range of [15]. This estimation reconfirms that a CSCNF is close in nature to a 1D harmonic chain with 3D oscillations. In addition, if $a^*/T^{*0.5}$ is 50, α should be about 0.85 according to [15]. The deviation between this value and ours (0.75) probably originates in the phonon scattering inside each cup produced by, for example, the breathing-like and original graphene modes discussed above.

6. Summary

Phonon transport in a CSCNF is treated using a molecular dynamics simulation. The thermal conductivity is found to obey the power law of $\lambda \propto L^{0.7}$, which has the highest exponent ever discovered at room temperature. In a CSCNF, low frequency axial and radial oscillations contribute to the heat conduction because the connection between cups is by van der Waals' forces. On the other hand, the low frequency circumferential mode is weak and propagates poorly due to free rotation of intermediate cups. The axial mode acts as if each cup behaves like a rigid body, but the radial mode originates in a breathing-like deformation of a cup. Because both modes are local oscillations, it can be concluded that a CSCNF is the most one-dimensional system in terms of phonon transport. This unique property of a CSCNF raises our hopes of transporting thermal energy without loss over a longer distance than ever.

Acknowledgment

This work was supported by a Grant-in-Aid for JSPS Fellows (21661).

References

[1] Hone J, Whitney M, Piskoti C and Zettl A 1999 *Phys. Rev.* B **59** R2514
[2] Hone J, Llanguno M C, Nemes N M, Johnson A T, Fischer J E, Walters D A, Casavant M J, Schmdit J and Smalley R E 2000 *Appl. Phys. Lett.* **77** 666
[3] Kim P, Shi L, Majumdar A and McEuen P L 2001 *Phys. Rev. Lett.* **87** 215502
[4] Fujii M, Zhang X, Xie H, Ago H, Takahashi K, Ikuta T, Abe H and Shimizu T 2005 *Phys. Rev. Lett.* **95** 065502
[5] Yu C, Shi L, Yao Z, Li D and Majumdar A 2005 *Nano Lett.* **5** 1842
[6] Berber S, Kwon Y K and Tománek D 2000 *Phys. Rev. Lett.* **84** 4613

[7] Osman M A and Srivastava D 2001 *Nanotechnology* **12** 21
[8] Mingo N and Broido D A 2005 *Nano Lett.* **5** 1221
[9] Maruyama S 2002 *Physica* B **323** 193
[10] Livi R and Lepri S 2003 *Nature* **421** 327
[11] Rieder Z, Lebowitz J L and Lieb E 1967 *J. Math. Phys.* **8** 1073
[12] Lepri S, Livi R and Politi A 1997 *Phys. Rev. Lett.* **78** 1896
[13] Lepli S 2000 *Eur. Phys. J.* B **18** 441
[14] Hatano T 1999 *Phys. Rev.* E **59** R1
[15] Liu Z and Li B 2008 *J. Phys. Soc. Japan* **77** 074003
[16] Zhang G and Li B 2005 *J. Chem. Phys.* **123** 114714
[17] Wang J and Wang J-S 2006 *Appl. Phys. Lett.* **88** 111909
[18] Chang C W, Okawa D, Garcia H, Majumdar A and Zettle A 2008 *Phys. Rev. Lett.* **101** 075903
[19] Wang Z L, Tang D W, Li X B, Zheng X H, Zhang W G, Zheng L X, Zhu Y T, Jin A Z, Yang H F and Gu C Z 2007 *Appl. Phys. Lett.* **91** 123119
[20] Shiomi J and Maruyama S 2008 *Japan. J. Appl. Phys.* **47** 2005
[21] Takahashi K, Ito Y, Ikuta T, Zhang X and Fujii M 2009 *Physica* B **404** 2431
[22] Endo M, Kim Y A, Hayashi T, Fukai Y, Oshiba K, Terrones M, Yanagisawa T, Higaki S and Dresselhaus M S 2002 *Appl. Phys. Lett.* **80** 1267
[23] Slack G A 1962 *Phys. Rev.* **127** 694
[24] Sun K, Stroscio M A and Dutta M 2009 *Superlatt. Microstruct.* **45** 60
[25] Brenner D W 1990 *Phys. Rev.* B **42** 9458
[26] Hoover W G 1985 *Phys. Rev.* A **31** 1695
[27] Kittel C 2005 *Introduction to Solid State Physics* 8th edn (New York: Wiley)
[28] Dumitricą T, Garcia M E, Jeschke H O and Yakobson B I 2006 *Phys. Rev.* B **74** 193406
[29] Hu B, Li B and Zhao H 1998 *Phys. Rev.* E **57** 2992
[30] Lepri S, Livi R and Politi A 2003 *Phys. Rep.* **377** 1